Pharmaceutical Sciences and Drug Design
ISSN: 3062-4428
2022, Volume 2, Page No: 130-144

Available online at: www.galaxypub.co/page/journals

Galaxy Publication

Galaxy Publication

Dehydrolithocholic Acid (DHLCA) Ameliorates Diabetic Kidney Disease by Activating TGR5/FXR Signaling and Remodeling the Gut Microbiota

Liam Wilson[1]*, Noah Baker[1], Ava Turner[1]

[1]Department of Biotechnology, Faculty of Medical Sciences, University of Queensland, Brisbane, Australia.

***E-mail** ✉ liam.wilson.au@hotmail.com

Received: 02 February 2022; **Revised:** 27 April 2022; **Accepted:** 02 May 2022

ABSTRACT

Diabetic kidney disease (DKD) is one of the primary causes of long-term loss of renal function internationally. In recent years, bile acids (BAs) have emerged as important metabolic signals influencing glucose control and kidney physiology. This project explored how disturbances in BA pathways contribute to DKD advancement. Plasma BA concentrations were quantified in healthy individuals (HC), subjects with type 2 diabetes mellitus (T2DM), and patients diagnosed with DKD using ultra-high-performance liquid chromatography coupled with tandem mass spectrometry (UPLC-MS/MS). After potential BA markers were identified in the clinical cohort, mechanistic validation was carried out in a DKD mouse model treated with dehydrolithocholic acid (DHLCA). Kidney injury indicators and the expression of Takeda G protein-coupled receptor 5 (TGR5) and farnesoid X receptor (FXR) were assessed. Metagenomic sequencing was also performed to characterize gut microbiota (GM) after DHLCA exposure.

DHLCA levels in plasma were markedly decreased in DKD patients with macroalbuminuria compared with both the T2DM group and the DKD cohort with microalbuminuria ($P < 0.01$). Partial Spearman analysis controlling for age and diabetes duration indicated a negative correlation between DHLCA and urinary albumin ($\rho = –0.347$; 95% CI, –0.531 to –0.135; $q = 0.008$), as well as with urine albumin-to-creatinine ratio (UACR) ($\rho = –0.332$; 95% CI, –0.499 to –0.155; $q = 0.010$). In vivo, DHLCA administration significantly reduced UACR and fasting blood glucose (FBG) levels ($P < 0.01$) and improved liver enzyme status (ALT, $P < 0.05$). DHLCA lowered renal tubular damage, restored normal TGR5 and FXR expression patterns, and decreased kidney injury molecule-1 (KIM-1) and neutrophil gelatinase-associated lipocalin (NGAL). Metagenomic analysis showed an increase in Lachnospiraceae bacterium after treatment. DHLCA may represent a useful DKD therapeutic candidate by engaging the FXR/TGR5 pathways and altering gut microbial composition. Its renal and metabolic improvements, together with enhanced liver safety and absence of hepatotoxicity, justify continued translational development.

Keywords: Bile acid, Diabetic kidney disease, Farnesoid X receptor, Gut microbiota, Takeda G protein-coupled receptor 5

How to Cite This Article: Wilson L, Baker N, Turner A. Dehydrolithocholic Acid (DHLCA) Ameliorates Diabetic Kidney Disease by Activating TGR5/FXR Signaling and Remodeling the Gut Microbiota. Pharm Sci Drug Des. 2022;2:130-44. https://doi.org/10.51847/2RLip6mpou

Introduction

Diabetes mellitus (DM) results in numerous organ complications, and diabetic kidney disease (DKD) is the most severe, often culminating in end-stage renal disease (ESRD) [1]. With current treatment options offering limited benefit, investigators are continuing to examine the underlying biological processes and identify new therapeutic targets.

Metabolomic findings have demonstrated progressive changes in bile acid (BA) profiles with advancing DKD, implying that BA abnormalities may not only track disease progression but also actively drive it [2]. BA activity is largely mediated through receptors such as the farnesoid X receptor (FXR) and Takeda G protein-coupled receptor 5 (TGR5) [3, 4]. FXR engagement has been documented to reduce diabetic kidney damage by influencing lipid handling, decreasing fibrosis and inflammation, and limiting oxidative stress [5]. TGR5 stimulation supports

mitochondrial function, boosts antioxidant pathways, and lessens diabetes-related renal injury [6]. However, how these receptors behave specifically in kidneys affected by DKD remains incompletely defined.

Growing data indicate that the interaction between gut microbiota (GM) and BAs is central to maintaining metabolic stability and renal health [3, 7–9]. Disruption of this GM-BA network may represent a mechanistic bridge linking intestinal dysbiosis to DKD progression [10]. Key unanswered questions include:

(i) how individual BAs behave across the clinical spectrum of DKD;

(ii) how GM-BA relationships influence receptor signaling inside the kidney; and

(iii) whether secondary BAs might serve as natural FXR/TGR5 agonists with therapeutic potential.

This study tested the idea that the secondary BA dehydrolithocholic acid (DHLCA) can reduce tubular injury and lower proteinuria in DKD by acting on both FXR and TGR5 while reshaping the gut microbiota. To our knowledge, this is the first investigation to combine patient profiling, BA metabolomics, microbiome characterization, and mechanistic evaluation of a single BA derivative in DKD, offering new evidence for endogenous BA-based kidney protection and future clinical strategies.

Materials and Methods

Patients

This forward-looking cohort study was performed at the Third Affiliated Hospital of Soochow University from April 2021 to August 2022. A total of 92 individuals with type 2 diabetes mellitus (T2DM) were consecutively enrolled, along with 31 healthy controls (HC) matched for age and sex. Eligibility for the T2DM group required:

(1) diagnosis consistent with the 2020 American Diabetes Association standards [11];

(2) age above 18 years;

(3) an estimated glomerular filtration rate (eGFR) of at least 90 mL/min/1.73 m² as calculated by CKD-EPI Creatinine [12].

Participants were excluded if they had:

(1) pregnancy or any form of malignancy;

(2) kidney disorders unrelated to diabetes;

(3) active inflammatory diseases involving the liver or intestinal tract.

Healthy controls were recruited only if they met the following:

(1) absence of hypertension, diabetes, or other chronic systemic disorders;

(2) no need for ongoing medication to manage long-term disease;

(3) routine biochemistry confirming normal glucose, renal, and hepatic findings.

T2DM subjects were separated into three subgroups based on urine albumin-to-creatinine ratio (UACR):

(1) normoalbuminuria (T2DM group; UACR < 30 mg/g; n = 31),

(2) clinically verified DKD with microalbuminuria (DKD micro group; 30 ≤ UACR ≤ 300 mg/g; n = 30),

(3) clinically verified DKD with macroalbuminuria (DKD macro group; UACR > 300 mg/g; n = 31).

To prevent metabolic bias related to impaired excretion, only participants with preserved renal performance (eGFR ≥ 90 mL/min/1.73 m²) were included.

The study received approval from the Ethics Committee of the Third Affiliated Hospital of Soochow University (Ethics No. 2021–136, approval date 2021–03-10). All procedures were aligned with the Declaration of Helsinki, and written informed consent was obtained from every participant.

Sample collection

After an overnight fast, 5 mL of venous blood was collected from each participant into EDTA anticoagulant tubes. Samples were centrifuged at 4000 rpm for 15 minutes, and the resulting plasma was preserved at −80°C until analysis.

Animal model

Thirty-one male C57BL/6J mice, 4 weeks old, were purchased from the Model Animal Research Center of Nanjing University (Nanjing, China). Animals were randomly assigned to experimental groups. All animal

handling was conducted according to institutional animal research standards and approved by the Ethics Committee of the Third Affiliated Hospital of Soochow University. Housing conditions were standardized at 24°C, 40–70% humidity, a 12-hour light/dark schedule, and proper air exchange.
Mice were divided into two dietary cohorts:

- a low-fat diet (LFD, 10%; n = 5),
- a high-fat diet (HFD, 60%; n = 26).

At week 14, HFD-fed mice received intraperitoneal streptozotocin (STZ) at 40 mg/kg for 5 consecutive days, while the LFD group received sodium citrate buffer on the same schedule. Diabetes was confirmed when fasting blood glucose (FBG) exceeded 11.1 mmol/L.
At week 18, after fasting overnight:

- control animals received oral CMC-Na for 2 weeks,
- diabetic mice were administered DHLCA at 5 mg/kg (n = 5), 10 mg/kg (n = 8), or 20 mg/kg (n = 5),
- the remaining diabetic mice received CMC-Na (n = 8).

At 20 weeks of age, all animals were euthanized, and tissues and fluids were collected for subsequent assays. Urinary creatinine (Hitachi automatic analyzer 3500) and urinary albumin (MedicalSystem) were assessed using routine laboratory procedures. Additional biochemical measurements included blood urea nitrogen (BUN), serum creatinine (Scr), urinary creatinine, alanine aminotransferase (ALT), aspartate aminotransferase (AST), and total bile acids (TBA), all analyzed on an automated Hitachi platform.

RNA extraction and RT-qPCR
Total RNA was isolated from renal tissue using Trizol reagent (Invitrogen, USA). The collected RNA was subsequently converted into cDNA with the PrimeScript™ RT reagent Kit (Takara, Japan), following the manufacturer's recommended workflow. Quantitative PCR was carried out on a Thermo Fisher Scientific system using SYBR Premix Ex Taq™ (Takara, Japan). The mouse primer sequences applied in this work (RiboBio, China) are listed in **Table 1**. β-actin served as the reference gene for normalization.

Table 1. Demographic and Clinical Characteristics of Participants

Parameter	Healthy Controls (n=31)	T2DM without DKD (n=31)	DKD with Microalbuminuria (n=30)	DKD with Macroalbuminuria (n=31)	P-value	FDR-adjusted q-value
Age (years)	50.0 (41.0, 59.0)	54.0 (47.0, 61.0)	51.5 (37.8, 70.0)	56.0 (51.0, 69.0)	0.156	0.189
Sex (male/female)	12/19	17/14	17/13	22/9	0.088	0.088
Diabetes duration (years)	–	4.0 (0.5, 10.0)	6.5 (1.0, 11.3)	10.0 (8.0, 15.0)#,†	<0.001	0.002
Body mass index (kg/m²)	–	23.2 (21.4, 25.3)	25.9 (23.4, 29.0)#	24.7 (22.3, 25.8)	0.007	0.018
White blood cell count (×10⁹/L)	5.2 (4.7, 6.2)	5.7 (5.0, 6.7)	6.3 (5.4, 7.9)*	7.2 (5.8, 9.1)*,#	<0.001	0.001
Red blood cell count (×10¹²/L)	4.6 (4.4, 4.8)	4.6 (4.3, 4.8)	4.6 (4.4, 5.2)	4.2 (3.7, 4.7)*,#,†	0.007	0.013
Hemoglobin (g/L)	138.0 (131.0, 145.0)	138.0 (125.0, 145.0)	139.5 (129.0, 153.3)	121.0 (111.0, 140.0)*,†	0.008	0.014
Neutrophil-to-lymphocyte ratio	1.8 (1.4, 2.3)	1.6 (1.3, 2.0)	1.7 (1.4, 2.1)	2.4 (1.7, 4.4)*,#,†	<0.001	0.002
Serum albumin (g/L)	44.9 (43.6, 46.4)	39.1 (37.5, 42.5)*	38.6 (36.9, 41.2)*	35.2 (32.1, 38.8)*,#,†	<0.001	<0.001
Blood urea nitrogen (mmol/L)	5.1 ± 1.3	5.1 ± 1.5	5.8 ± 1.9	5.6 ± 1.8	0.249	0.249
Serum creatinine (μmol/L)	63.1 ± 9.8	56.7 ± 10.5*	62.9 ± 8.3#	65.2 ± 10.4#	0.006	0.009
eGFR (mL/min/1.73 m²)	102.6 (94.9, 111.8)	112.5 (103.4, 133.2)*	110.8 (91.3, 121.2)	97.7 (93.9, 105.0)#,†	<0.001	0.001

Urinary albumin concentration (mg/L)	13.3 (9.4, 21.8)	12.1 (8.3, 14.9)	68.7 (29.3, 133.8)*,#	667.1 (450.4, 1235.0)*,#,†	<0.001	<0.001
Urine albumin-to-creatinine ratio (mg/g)	9.7 (7.1, 10.6)	10.7 (7.8, 19.2)	84.0 (40.3, 154.1)*,#	928.1 (520.0, 1426.6)*,#,†	<0.001	<0.001
Total cholesterol (mmol/L)	4.6 (3.9, 5.3)	4.9 (3.8, 5.4)	5.0 (3.9, 5.6)	4.4 (3.5, 5.6)	0.776	0.851
Triglycerides (mmol/L)	1.0 (0.8, 1.5)	1.3 (1.1, 2.5)*	2.2 (1.5, 3.3)*	1.7 (1.1, 2.7)*	<0.001	<0.001
HDL cholesterol (mmol/L)	1.5 (1.2, 1.7)	1.1 (1.0, 1.3)*	1.0 (0.8, 1.1)*,#	1.0 (0.8, 1.2)*	<0.001	<0.001
LDL cholesterol (mmol/L)	2.6 (2.1, 3.1)	2.7 (1.8, 3.1)	2.5 (2.1, 3.2)	2.5 (2.0, 3.0)	0.893	0.907
HbA1c (%)	–	8.2 (7.8, 10.5)	9.0 (7.3, 11.0)	10.4 (8.2, 11.9)	0.226	0.226
Fasting blood glucose (mmol/L)	5.0 ± 0.4	9.1 ± 3.4*	10.1 ± 3.5*	10.8 ± 4.3*	<0.001	<0.001
Fasting C-peptide (ng/mL)	–	498.7 (346.4, 560.0)	661.5 (529.2, 837.3)#	486.7 (345.8, 743.2)	0.009	0.018
Alanine aminotransferase (U/L)	17.7 (15.0, 22.3)	19.1 (14.3, 23.1)	21.5 (13.4, 68.8)	17.4 (11.6, 29.2)	0.529	0.591
Aspartate aminotransferase (U/L)	23.1 (18.6, 27.1)	17.6 (14.7, 22.0)	20.7 (14.4, 40.0)	16.2 (14.3, 26.2)	0.050	0.073
Gamma-glutamyl transferase (U/L)	18.7 (14.4, 29.4)	22.7 (14.6, 28.5)	31.3 (16.8, 59.2)*	22.2 (18.1, 37.5)	0.029	0.044
Alkaline phosphatase (U/L)	75.0 (63.0, 97.0)	73.0 (65.0, 89.0)	79.0 (68.0, 98.0)	97.0 (69.0, 118.0)	0.126	0.163
Lactate dehydrogenase (U/L)	–	143.0 (135.0, 162.0)	171.0 (155.0, 204.3)#	175.0 (153.0, 196.0)#	<0.001	0.002
Adenosine deaminase (U/L)	–	12.4 (10.3, 15.1)	14.5 (11.8, 19.0)	15.9 (12.6, 22.4)#	0.014	0.023
Cholinesterase (U/L)	–	8850.0 (7221.0, 10,548.0)	9179.0 (7419.3, 11,101.8)	7301.0 (5967.0, 10,088.0)	0.069	0.083
Total bile acids (μmol/L)	–	3.7 (2.3, 6.6)	4.7 (2.6, 7.8)	2.8 (1.6, 5.8)	0.073	0.083
Total bilirubin (μmol/L)	13.3 (9.7, 17.8)	12.6 (9.0, 15.0)	12.9 (10.7, 14.0)	9.2 (7.3, 11.9)*,#,†	0.002	0.005
Direct bilirubin (μmol/L)	4.4 (2.9, 5.2)	3.9 (2.9, 4.6)	3.8 (3.2, 5.0)	3.0 (2.5, 4.4)	0.083	0.112
Indirect bilirubin (μmol/L)	9.3 (6.8, 12.6)	8.5 (6.1, 10.6)	8.5 (6.9, 9.8)	5.9 (4.7, 6.6)*,#,†	<0.001	0.001

Notes: *FDR-q < 0.05 vs HC group; #FDR-q < 0.05 vs T2DM group; †FDR-q < 0.05 vs DKD micro group. Abbreviations: HC, healthy control; DM, diabetes mellitus; DKD, diabetic kidney disease; FDR, false discovery rate; BMI, body mass index; WBC, white blood cell; RBC, red blood cell; Hb, hemoglobin; NLR, neutrophil-to-lymphocyte ratio; ALB, albumin; BUN, blood urea nitrogen; Scr, serum creatinine; eGFR, estimated glomerular filtration rate; UACR, urine albumin-to-creatinine ratio; TC, total cholesterol; TG, triglycerides; HDL, high-density lipoprotein; LDL, low-density lipoprotein; HbA1c, hemoglobin A1c; FBG, fasting blood glucose; FCP, fasting C-peptide; ALT, alanine aminotransferase; AST, aspartate aminotransferase; GGT, gamma-glutamyl transferase; ALP, alkaline phosphatase; LDH, lactate dehydrogenase; ADA, adenosine deaminase; CHE, cholinesterase; TBA, total bile acid; TBIL, total bilirubin; DBIL, direct bilirubin; IBIL, indirect bilirubin.

Western blot

Renal proteins were extracted with radioimmunoprecipitation assay (RIPA) buffer, and the total protein concentration was determined using a bicinchoninic acid (BCA) assay. Proteins were separated and analyzed by Western blot. Before adding primary antibodies targeting TGR5 (ab72608, Abcam, USA), FXR (sc-25309, Santa Cruz, USA), and β-actin (MA1-140, Invitrogen, USA), membranes were incubated in 5% bovine serum albumin (BSA) to reduce non-specific binding. Blots were visualized and quantified using ImageJ software, and signal intensity was normalized to β-actin.

Histological, immunohistochemical, and immunofluorescence assessment

Kidney samples were preserved in 4% formaldehyde for 48 hours, then dehydrated and paraffin-embedded. Sections (4 μm) were cut and stained with hematoxylin–eosin (H&E), periodic acid-Schiff (PAS), and Masson's trichrome. For immunohistochemistry, antigen retrieval was carried out in nitrate buffer at 96°C for 10 minutes. Slides were blocked with 3% BSA for 30 minutes at room temperature, then incubated overnight at 4°C with primary antibodies to TGR5 and FXR. After incubation with suitable secondary antibodies, color development was completed using 3,3′-diaminobenzidine (Servicebio, China).

Tubulointerstitial injury was graded using the interstitial fibrosis and tubular atrophy (IFTA) scoring method:

0 = no IFTA;

1 = <25% involvement;

2 = 25–50%;

3 = ≥50% [13].

All microscopic evaluations were conducted by observers blinded to group identity to prevent interpretation bias.

Plasma metabolite profiling

Plasma bile acid metabolites were quantified with ultrahigh-performance liquid chromatography coupled to tandem mass spectrometry (UPLC-MS/MS) using a targeted metabolomics approach. Samples stored at −80°C were thawed on ice. Next, 50 μL of plasma and 300 μL of extraction solvent (1:1 acetonitrile: methanol with internal standards) were mixed in 2 mL tubes, vortexed for 3 minutes, and centrifuged for 15 minutes at 12,000 rpm and 4°C. A 200 μL supernatant fraction was transferred and kept at −20°C for 1 hour to precipitate proteins; then 180 μL was used for UPLC-MS/MS analysis.

Metagenomic sequencing and processing

Fecal DNA was isolated with the FastDNA SPIN Kit (MP Biomedicals, USA). Concentration and purity were evaluated with the Qubit™ dsDNA assay (Invitrogen, USA). Library preparation was performed with 200 ng DNA using the TruSeq DNA Nano Kit (Illumina), followed by paired-end sequencing on the NovaSeq 6000 platform. Raw reads were cleaned of adapters and low-quality bases using Cutadapt and Fqtrim, and host sequences were removed using Bowtie2. High-quality reads were assembled with MEGAHIT, genes were predicted, and redundant entries were eliminated to form a non-duplicate gene catalog. Protein sequences were aligned to the NCBI NR database through DIAMOND for taxonomic classification. Microbial groups with significant differences were identified using LEfSe (LDA > 3, $P < 0.05$).

Data and statistical analysis

All analytical procedures were carried out using three software platforms: R (v4.5.0; R Core Team, 2025), SPSS (v25.0; IBM Corp., Armonk, NY, USA, 2017), and GraphPad Prism (v9.0; GraphPad Software, San Diego, CA, USA, 2022). Normality of continuous variables was examined with the Kolmogorov–Smirnov test. Categorical outcomes were recorded as simple frequencies. If a variable followed a normal distribution, values were shown as mean ± standard deviation (SD); otherwise, median and interquartile range (IQR) were presented. Comparisons among more than two groups employed one-way ANOVA for parametric data and the Kruskal–Wallis H test when assumptions for parametric testing were not met. When global significance was detected ($P < 0.05$), post hoc analysis proceeded with Tukey (ANOVA) or Dunn (Kruskal–Wallis). To control for multiple hypothesis testing in omics-based datasets, including bile acid and gut microbiome measurements, false discovery rate (FDR) adjustment was applied. The chi-square test, also corrected with FDR where relevant, was used to compare categorical variables among groups. Nonlinear regression in GraphPad Prism was used to construct FBG and UACR dose–response curves from median ± SD data. For RT-qPCR and Western blot (n = 3 per group), one-way ANOVA combined with 1000 bootstrap resamples generated bias-corrected and accelerated 95% confidence intervals, and Tukey tests were used for subsequent group comparisons. Associations between clinical variables and bile acid levels were quantified using partial Spearman coefficients controlling for age and duration of diabetes. Two-sided P values were corrected using FDR adjustment, and 95% confidence intervals were derived from 1000 bootstrap iterations. Diagnostic discrimination was assessed using receiver operating characteristic (ROC) curves with area under the curve (AUC). Significance thresholds were set at two-sided $P < 0.05$ or FDR-$q < 0.05$.

Results and Discussion

Changes in circulating bile acids in DKD

Plasma bile acid profiles were quantified by UPLC-MS/MS. Group-level clinical characteristics appear in **Table 1**. Individuals classified in the DKD macro subgroup showed higher urine albumin, UACR, and neutrophil-to-lymphocyte ratio (NLR), while serum albumin (ALB), red blood cell counts (RBC), total bilirubin (TBIL), and indirect bilirubin (IBIL) were lower than in the other three groups ($P < 0.05$, **(Table 1)**).

In total, 50 bile acids were detected. The resulting metabolomics matrix was normalized and analyzed using MetaboAnalyst. A heat map illustrating group-wise differences is shown in **Figure 1**. Five primary bile acids—nor cholic acid (NCA), cholic acid (CA), glycochenodeoxycholic acid-3-sulfate (GCDCA-3S), chenodeoxycholic acid-3-β-D-glucuronide (CDCA-3Gln), and glycochenodeoxycho lic acid-3-O-β-glucuronide (GCDCA-3Gln)—as well as six secondary bile acids (DHLCA, lithocholic acid [LCA], deoxycholic acid [DCA], 3-dehydrocholic acid [3DHCA], glycolithocholic acid [GLCA], and taurolithocholic acid [TLCA]) differed significantly across HC, T2DM, DKD micro, and DKD macro groups, all with FDR-$q < 0.05$. Box plots showing group-to-group variations appear in **Figures 2a and 2b**.

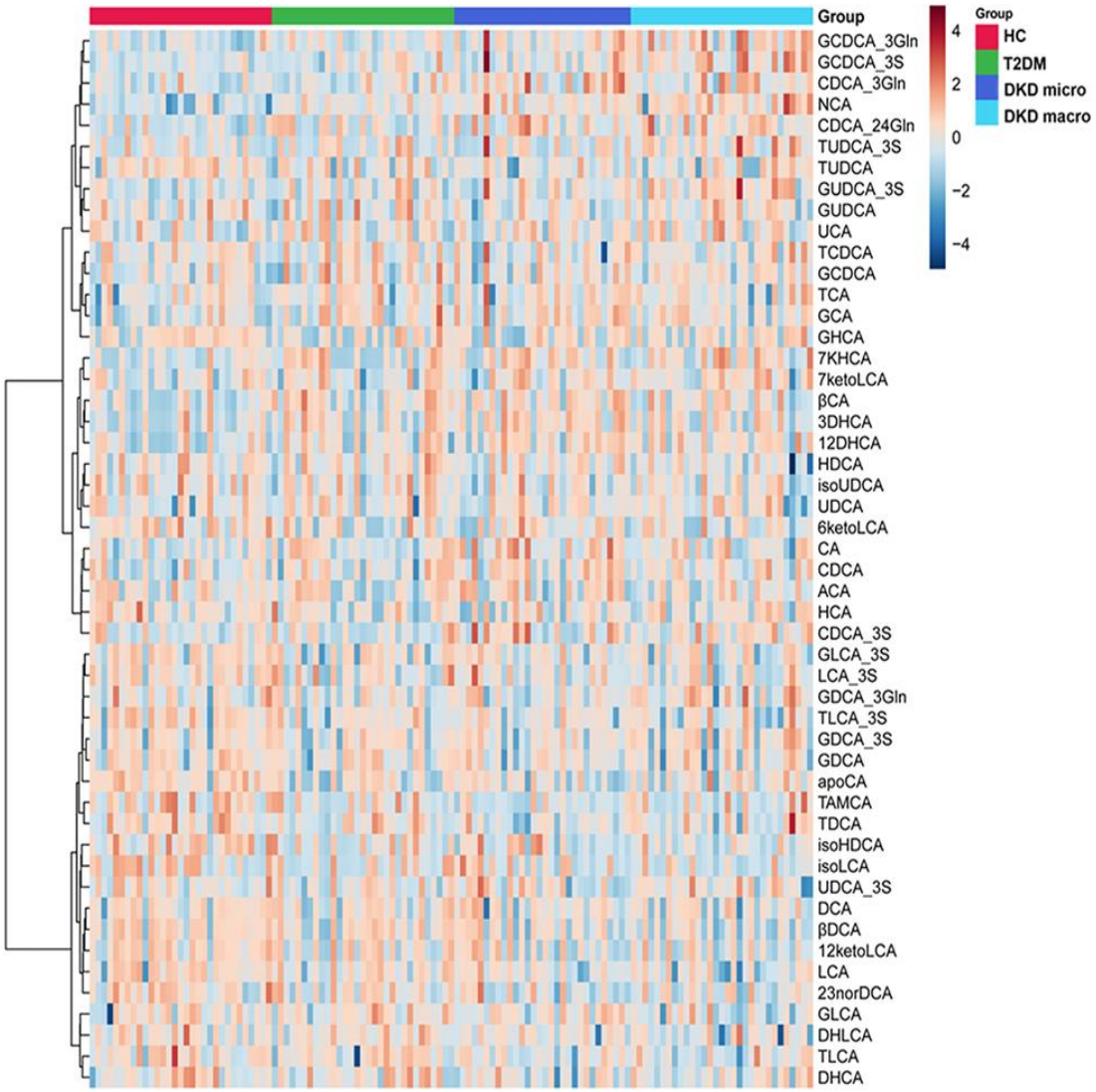

Figure 1. Metabolite heat map across the four groups. Columns correspond to individual samples, while rows denote the metabolites, with color indicating their relative abundance. The heat map illustrates metabolite patterns among the HC group, T2DM group, DKD micro group, and DKD macro group.

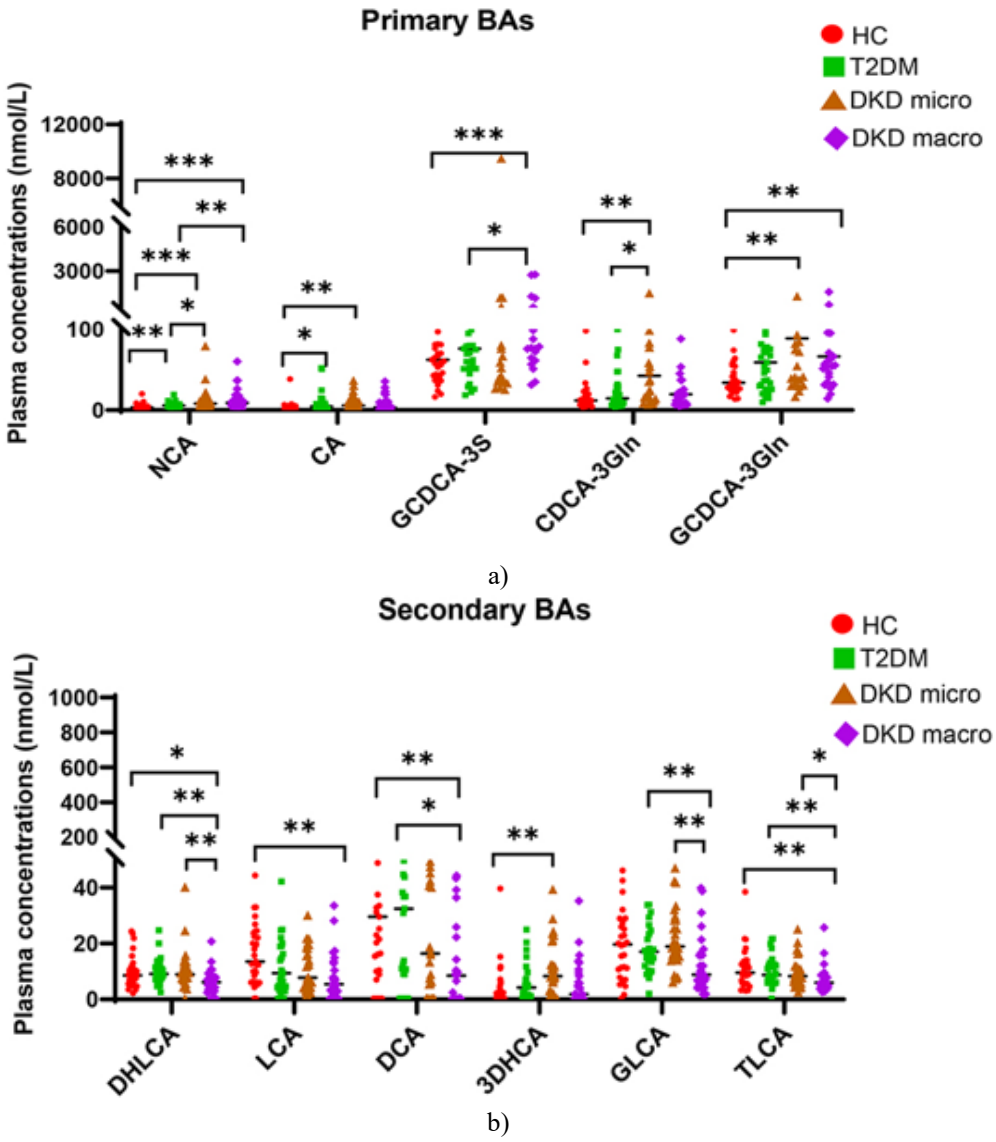

Figure 2. Plasma bile acid concentrations: (a) primary bile acids, (b) secondary bile acids. *Significance: *FDR-q < 0.05; **FDR-q < 0.01; **FDR-q < 0.001.

Partial spearman correlations between bile acids and clinical features

Partial Spearman correlation analysis, adjusted for both diabetes duration and age, was carried out for the 11 bile acids that differed among groups. FDR correction was applied **(Figure 3)**. Three secondary bile acids—DHLCA, TLCA, and GLCA—were consistently and negatively associated with urine albumin output. DHLCA showed inverse correlations with urine albumin ($\rho = -0.347$; 95% CI, –0.531 to –0.135; $q = 0.008$) and UACR ($\rho = -0.332$; 95% CI, –0.499 to –0.155; $q = 0.010$). TLCA was similarly associated with both urine albumin ($\rho = -0.416$; 95% CI, –0.563 to –0.250; $q = 0.001$) and UACR ($\rho = -0.374$; 95% CI, –0.554 to –0.188; $q = 0.003$). GLCA demonstrated the same pattern, correlating negatively with urine albumin ($\rho = -0.324$; 95% CI, –0.520 to –0.114; $q = 0.012$) and UACR ($\rho = -0.329$; 95% CI, –0.533 to –0.125; $q = 0.011$). Collectively, these correlations indicate that lower circulating concentrations of several secondary bile acids are linked with greater albuminuria severity in DKD.

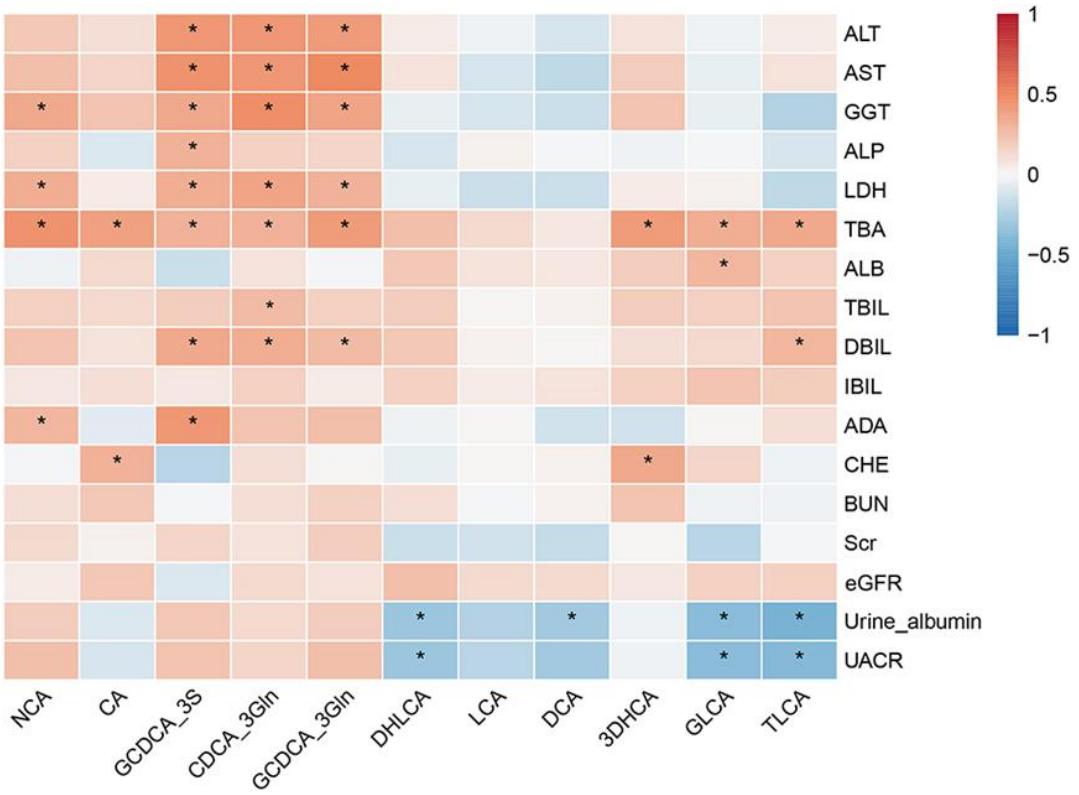

Figure 3. Association Between Clinical Parameters and BAs Metabolites
FDR-q < 0.05.

Diagnostic performance of DHLCA for albuminuria

To determine whether plasma DHLCA can differentiate macroalbuminuria from microalbuminuria in DKD patients, ROC assessment was carried out. DHLCA produced an AUC of 0.738 (95% CI: 0.609–0.867), representing a moderate classification ability **(Figure 4)**.

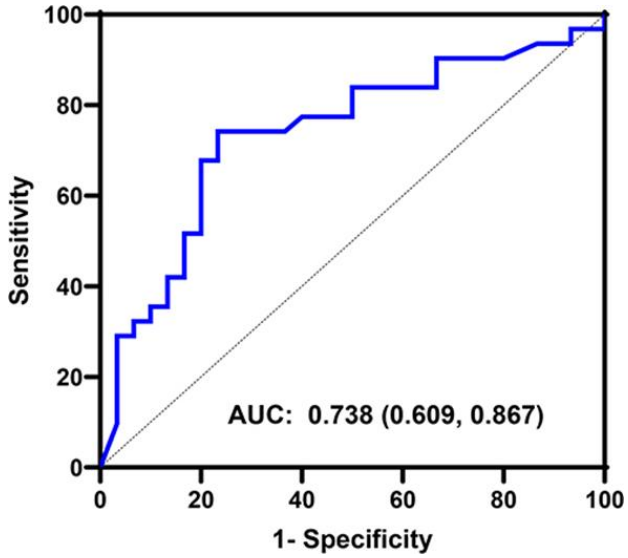

Figure 4. ROC evaluation of DHLCA in DKD with macroalbuminuria.

Impact of DHLCA administration in DKD

STZ-induced mice were treated with DHLCA at 5, 10, or 20 mg/kg. After 20 weeks, the 10 mg/kg group demonstrated the most substantial gains in renal function and metabolic control, including reduced UACR, fasting blood glucose, IFTA severity, and downregulation of tubular injury proteins KIM-1 and NGAL. Dose analysis showed improvement increased up to 10 mg/kg, with no further benefit at higher doses. Consequently, 10 mg/kg

was selected for the primary analyses. Comparative findings for control, DKD, and DHLCA-treated DKD animals are shown in **Figure 5**.

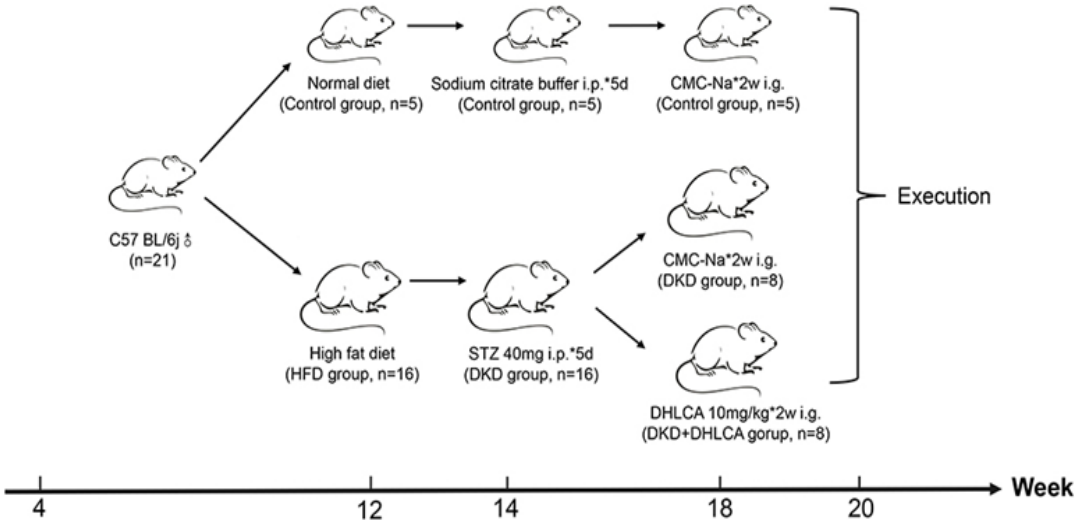

Figure 5. DHLCA-treated DKD mouse groups.

Compared with the DKD group, mice receiving DHLCA exhibited significant decreases in UACR, kidney weight/body weight ratio, TBA, and FBG at 20 weeks ($P < 0.05$, **(Figures 6a and 6h)**). In contrast, creatinine clearance (Ccr) and BUN were unchanged ($P > 0.05$, **(Figures 6b and 6c)**).

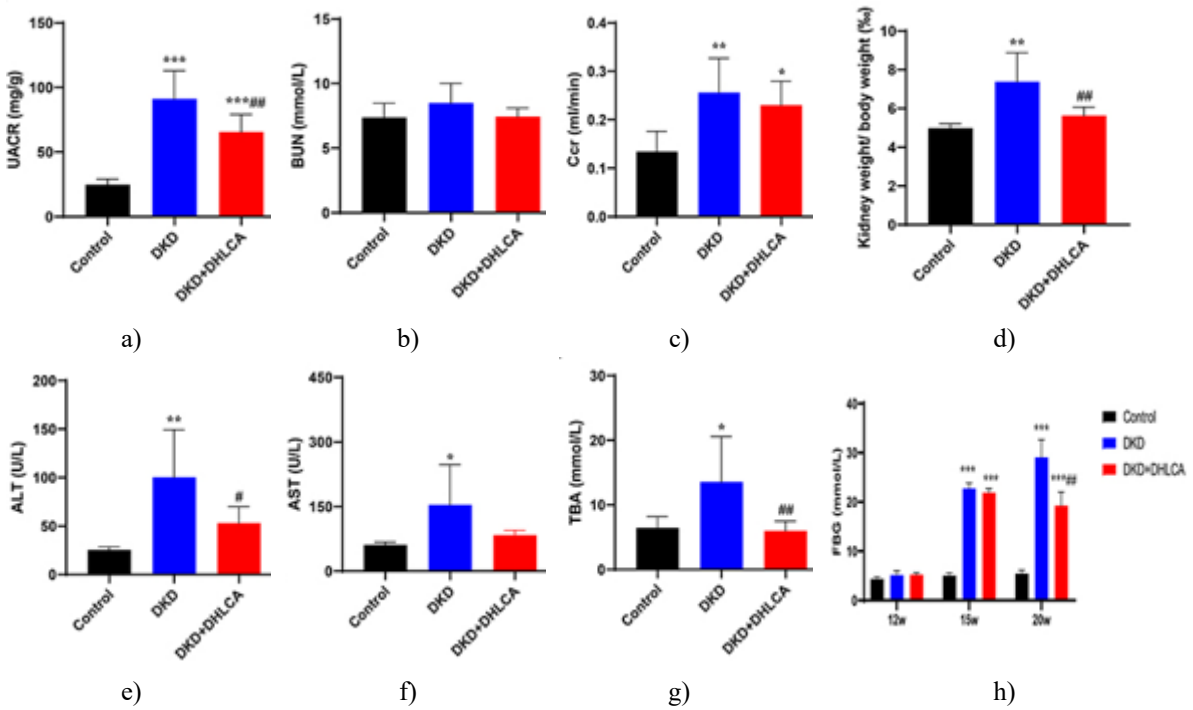

Figure 6. DHLCA Modifies Renal and Hepatic Profiles

(a) UACR. (b) BUN. (c) Ccr. (d) Kidney weight/body weight. (e) ALT. (f) AST. (g) TBA. (h) FBG. *P < 0.05 vs Control; **P < 0.01 vs Control; **P < 0.001 vs Control; #P < 0.05 vs DKD; ##P < 0.01 vs DKD.

For liver parameters, DKD animals showed elevated ALT and AST compared with controls ($P < 0.05$, **(Figures 6e and 6f)**). DHLCA treatment led to a significant reduction in ALT compared with the untreated DKD group ($P < 0.05$, **(Figure 6e)**), demonstrating a protective effect on hepatic function.

H&E, PAS, and Masson staining confirmed that DHLCA lessened tubular lesions in DKD. The IFTA score was lower in DHLCA-treated mice than in DKD animals ($P < 0.05$, **(Figures 7a–7b)**). DHLCA also reduced the expression of KIM-1 and NGAL **(Figure 7c)**. Immunostaining further indicated that DHLCA markedly elevated TGR5 and FXR in renal tubular epithelial cells **(Figure 7e)**. Corresponding increases in mRNA and protein levels of TGR5 and FXR were likewise observed ($P < 0.05$, **(Figures 7d, 7g and Table 2)**).

Table 2. Primer Sequences

Gene	Species	Forward Primer (5′ → 3′)	Reverse Primer (5′ → 3′)
β-actin	Mouse	TCAAGATCATTGCTCCTCCTGAG	ACATCTGCTGGAAGGTGGACA
Tgr5	Mouse	CTCTACCTGGAAGTTTATGGCCT	AGTCGGCGGATCTCACACA
Fxr	Mouse	TGTACCAGCCTGAGAACCCG	TGTGATCATTCACTCTCCAAGACAT

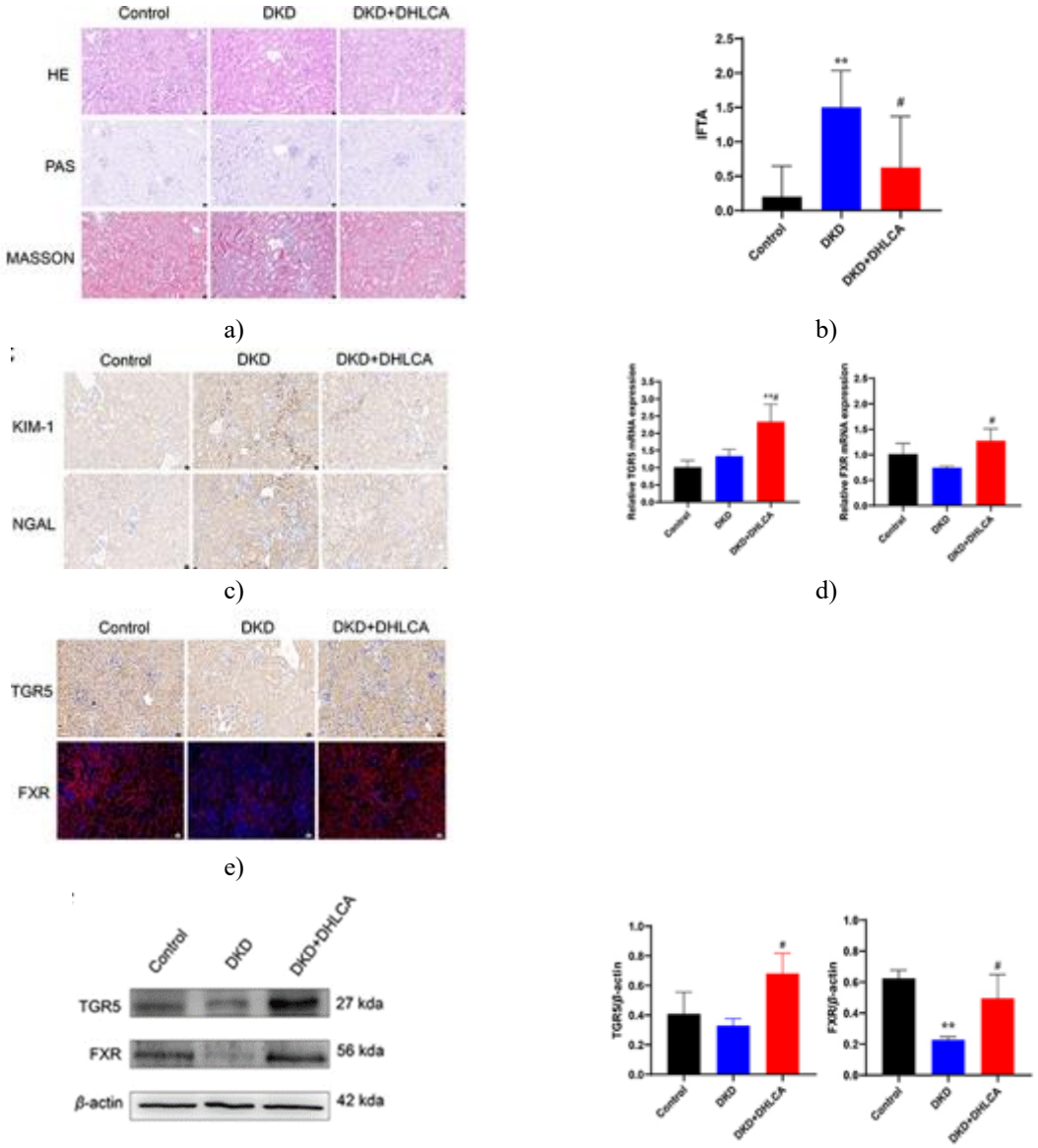

Figure 7. DHLCA Improves Tubular Renal Pathology

(a) Renal micrographs (H&E, PAS, Masson; magnification 40×; Control n = 5, DKD n = 8, DHLCA n = 8).

(b) IFTA quantification (same group sizes and magnification).

(c) Immunostaining for KIM-1 and NGAL (same group sizes).

(d) RT-qPCR showing TGR5 and FXR expression (n = 3).

(e) TGR5 immunohistochemistry and FXR immunofluorescence (40×; identical sample sizes).

(f) Western blot of TGR5 and FXR (n = 3).
(g) Quantification of western blot signals normalized to β-actin (n = 3).
P < 0.01 vs Control; #P < 0.05 vs DKD.

Effect of DHLCA on gut microbiota in DKD

Metagenomic profiling was conducted to identify microbial changes associated with DHLCA exposure. A taxonomic phylogram illustrated community shifts across seven taxonomic levels, including domain through species **(Figure 8a)**. Microbes with LDA > 3 and P < 0.05 are displayed in **Figure 8b**. Seventeen differential species were detected by LEfSe.

As shown in **Figure 8c**, DHLCA treatment increased several Lachnospiraceae taxa (Lachnospiraceae bacterium M18-1, 3-1, MD308, 28-4, and Acetatifactor muris), along with Bacteroides acidifaciens, several Firmicutes strains (ASF500 and Eubacterium sp. CAG:180), Bacterium 1xD42-87, Bacterium 1xD42-67, and Acutalibacter sp. 1XD8-33. Meanwhile, reductions were noted in Akkermansia muciniphila, Muribaculaceae unclassified, Bacteroidales unclassified, Bacteroidales bacterium, and Muribaculaceae bacterium Isolate-037 (Harlan).

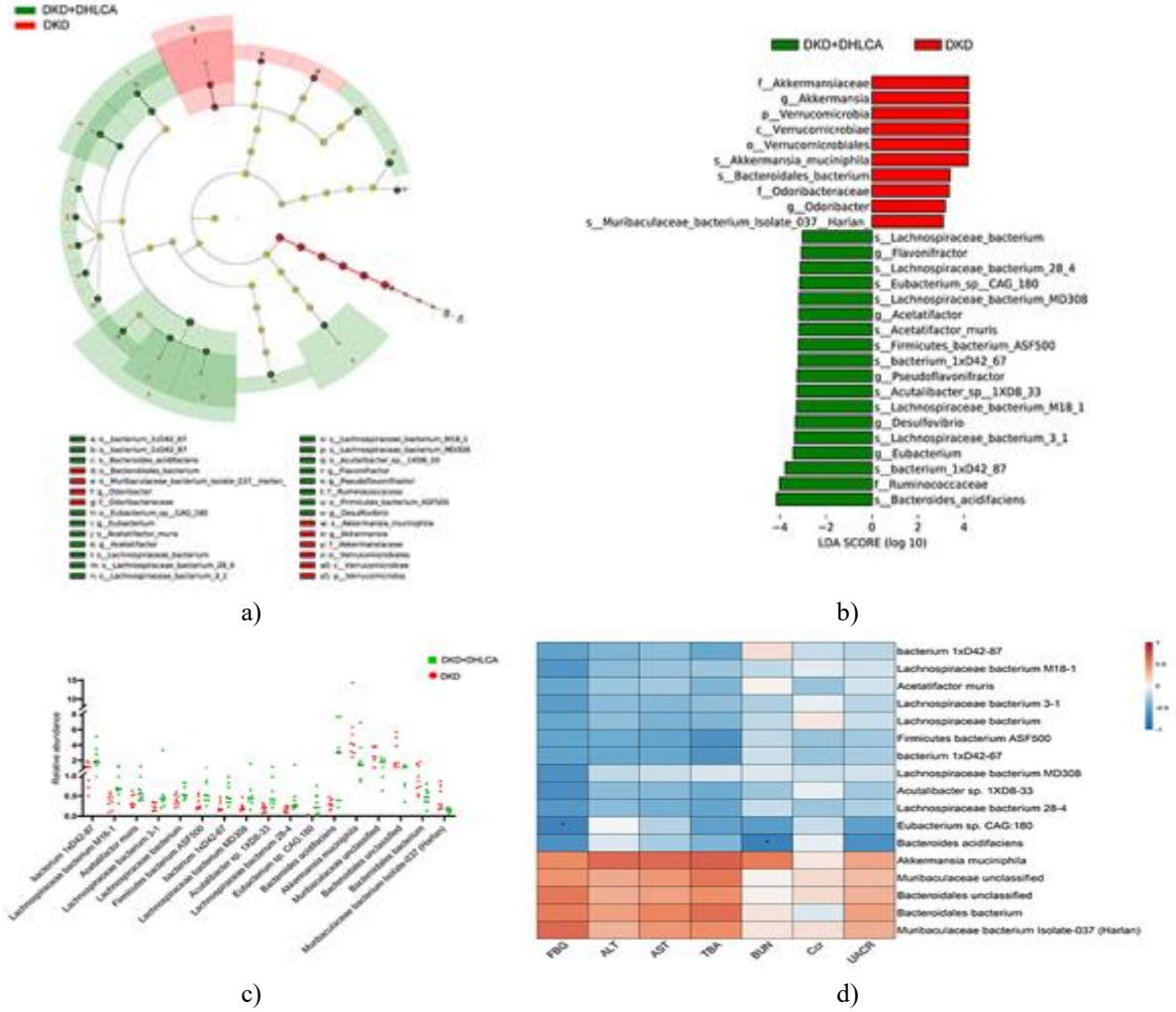

Figure 8. DHLCA alters GM composition.
(a) Comparative phylogenetic analysis of mice in the DKD group versus the DKD+DHLCA group.
(b) A bar chart highlighting microbial taxa with LDA scores > 3 and P < 0.05.
(c) Species-level distinctions in GM profiles between DKD and DKD+DHLCA mice.
(d) Association matrix between GM and biochemical readouts. FDR-q < 0.05.

Connections among BAs, GM, and biochemical indicators

To clarify how metabolic traits in the host relate to GM after DHLCA administration, we conducted partial Spearman correlations linking serum biochemical markers with fecal microbial taxa, applying FDR correction.

Several notable relationships emerged: Muribaculaceae bacterium Isolate-037 (Harlan) and Bacteroidales bacterium were strongly and positively related to both FBG and UACR, implying their potential involvement in heightened glycemia and renal dysfunction. In contrast, Eubacterium sp. CAG:180 and Bacteroides acidifaciens showed pronounced negative correlations with FBG and UACR, suggesting a possible protective contribution under DHLCA treatment **(Figure 8d)**.

To further examine how DHLCA influences both GM and secondary BA metabolism, correlations were evaluated between six major fecal secondary BAs and microbial taxa, again using Spearman analysis with FDR adjustment. Distinct association patterns were detected: Lachnospiraceae bacterium MD308 and Lachnospiraceae bacterium M18-1 exhibited strong positive relationships with fecal DHLCA **(Figure 9)**, whereas Muribaculaceae bacterium Isolate-037 (Harlan) showed a marked negative trend **(Figure 9)**. Although none of these patterns achieved significance after FDR correction, they point to microbial taxa that may participate in the gut metabolic response triggered by DHLCA.

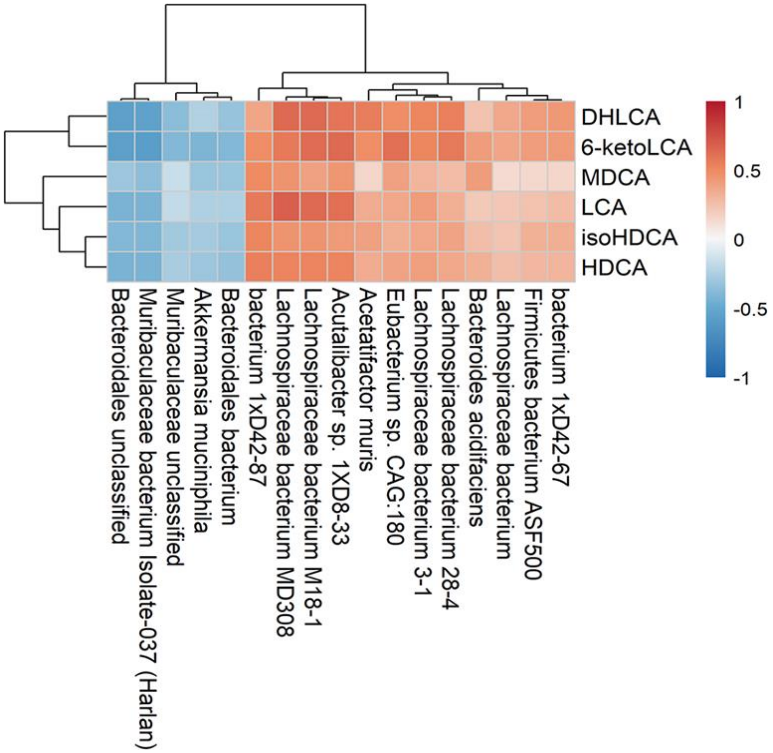

Figure 9. Heat map and correlation clustering between GM and BAs.

DKD represents a major diabetic complication and remains a leading cause of ESRD. Disturbances in metabolic pathways contribute substantially to its onset [14]. Metabolomics provides distinctive metabolic signatures that support disease prediction and diagnostic evaluation [15]. Although both TGR5 and FXR have been proposed as therapeutic targets in kidney disease linked to obesity and diabetes, upstream regulatory mechanisms remain insufficiently characterized. Our findings reveal stage-dependent alterations in BA metabolism in DKD. Plasma DHLCA showed an inverse relationship with albuminuria, and supplementation with DHLCA activated TGR5 and FXR, improving tubular injury, UACR, FBG, and GM composition in DKD mice.

Altered BA regulation is a defining feature of DKD, and we observed progressive shifts in plasma BA composition paralleling albuminuria severity. DHLCA levels were reduced in individuals with macroalbuminuria and were negatively associated with urinary albumin excretion, suggesting that loss of this BA may contribute to disease advancement. In STZ-induced DKD mice, DHLCA restored renal expression of TGR5 and FXR, alleviated tubular damage, and decreased UACR, indicating that its renoprotective action depends on dual receptor activation.

TGR5 and FXR modulate lipid and glucose balance, mitochondrial stability, oxidative injury, and fibrotic signaling; simultaneous activation therefore offers compounded benefits. The dual agonist INT-767 has been reported to reduce proteinuria and renal fibrosis in DKD models, emphasizing the therapeutic potential of targeting both receptors [16]. Across metabolic conditions, TGR5 enhances glucose utilization and energy expenditure,

whereas FXR governs BA homeostasis and limits inflammation—processes that collectively counteract obesity, diabetes, and DKD [16–22]. Taken together, our results support DHLCA as an endogenous dual-acting molecule that stimulates TGR5/FXR signaling and mitigates metabolic and inflammatory pathways central to DKD progression.

Altered GM profiles have been reported during the early development of DKD [23, 24], and accumulating data indicate that BAs and GM interact in a two-way regulatory manner [25]. In this work, we examined fecal samples from both DKD and DKD+DHLCA mice to further characterize BA–GM associations. Our analysis showed that DHLCA altered the overall GM landscape, notably increasing the relative abundance of Lachnospiraceae in the DKD+DHLCA group. Members of the Lachnospiraceae family produce short-chain fatty acids (SCFAs) with immunomodulatory effects [26], and have been linked to DM [27] as well as DKD [28]. The enrichment of this group after DHLCA treatment suggests that DHLCA may indirectly adjust GM composition to support improvement in DKD. We also observed a marked increase in Bacteroides acidifaciens following DHLCA administration. This species has been reported to protect against obesity and enhance insulin responsiveness in mouse models [29]. How these microbial shifts influence DKD outcomes after DHLCA exposure remains unresolved; isolating and transferring individual bacterial strains may help address this in future studies.

DM is characterized by impaired regulation of glucose and lipid metabolism and often progresses to secondary conditions such as NAFLD. Hepatic involvement in DM frequently results in elevated ALT and AST due to compromised liver function [30]. In our study, DHLCA reduced serum ALT in DKD mice, suggesting an unreported hepatoprotective effect. As a BA derivative, DHLCA influences both metabolic and immunological pathways. It suppresses Th17 differentiation and reduces IL-17A secretion [31], thereby lessening immune-mediated hepatic injury [32]. At the same time, DHLCA enhances insulin sensitivity through activation of FXR and TGR5 pathways [33, 34], limiting metabolic stress-driven hepatocellular damage. Together, these mechanisms likely underlie the decrease in ALT observed in our model. These findings led us to propose that DHLCA may provide liver-related benefits in addition to its renoprotective actions in DKD. Further targeted experiments will be required to confirm this hypothesis and delineate the specific biological pathways involved.

The present study provides new insight into the therapeutic potential of DHLCA in DKD; however, several limitations should be considered. First, the experimental scale was small, involving n = 3 biological replicates per group for RT-qPCR and WB and a clinical cohort of n = 122, thereby limiting statistical robustness. As such, molecular findings should be viewed as preliminary pending validation in larger datasets. Second, the cohort originated from a single center in China, restricting broader applicability; unaccounted factors such as diet, medications, and comorbidities may also have influenced BA changes. Multicenter investigations controlling for these variables will be essential. Third, efficacy was evaluated at a single time point using surrogate indices of early DKD rather than definitive renal outcomes. Longitudinal sampling and extended follow-up would strengthen interpretation. Fourth, the study lacks in vitro confirmation of DHLCA-driven TGR5 or FXR activation. Planned cellular experiments will be necessary to verify receptor engagement and define direct effects on tubular epithelial protection. Fifth, functional information at the species level was not available, limiting mechanistic understanding of how individual microbes contribute to BA and SCFA metabolic pathways. Establishing causal relationships among GM alterations, BA regulation, and renal benefit will require advanced functional and causal-inference approaches. Finally, a complete safety assessment of DHLCA—particularly regarding off-target actions in tissues expressing FXR or TGR5—is still needed. Pharmacokinetic profiling and long-term safety evaluations will be important for supporting its translational potential.

Conclusion

In conclusion, the study demonstrates that DHLCA mitigates DKD progression by engaging the TGR5/FXR axis and reshaping GM composition. DHLCA did not exhibit hepatotoxic effects and was instead associated with improved hepatic markers. These findings highlight DHLCA as a promising and potentially safe therapeutic option for DKD, meriting continued investigation in both preclinical and clinical models.

Acknowledgments: None

Conflict of Interest: None

Financial Support: None

Ethics Statement: None

References

1. Jager KJ, Kovesdy C, Langham R, Rosenberg M, Jha V, Zoccali C, et al. A single number for advocacy and communication-worldwide more than 850 million individuals have kidney diseases. Kidney Int. 2019;96(5):1048–50. doi:10.1016/j.kint.2019.07.012
2. Zhang Q, Lu L, Wang J, Lu M, Liu D, Zhou C, et al. Metabolomic profiling reveals the step-wise alteration of bile acid metabolism in patients with diabetic kidney disease. Nutr Diabetes. 2024;14(1):85. doi:10.1038/s41387-024-00315-0
3. Li Z, Yuan H, Chu H, Yang L, et al. The crosstalk between gut microbiota and bile acids promotes the development of non-alcoholic fatty liver disease. Microorganisms. 2023;11:2059. doi:10.3390/microorganisms11082059
4. Thibaut MM, Bindels LB. Crosstalk between bile acid-activated receptors and microbiome in entero-hepatic inflammation. Trends Mol Med. 2022;28(3):223–36. doi:10.1016/j.molmed.2021.12.006
5. Gai Z, Gui T, Hiller C, Kullak-Ublick GA. Farnesoid X receptor protects against kidney injury in uninephrectomized obese mice. J Biol Chem. 2016;291(5):2397–411. doi:10.1074/jbc.M115.694323
6. Wang XX, Edelstein MH, Gafter U, Qiu L, Luo Y, Dobrinskikh E, et al. G protein-coupled bile acid receptor TGR5 activation inhibits kidney disease in obesity and diabetes. J Am Soc Nephrol. 2016;27(5):1362–78. doi:10.1681/ASN.2014121271
7. Chen B, Bai Y, Tong F, Yan J, Zhang R, Zhong Y, et al. Glycoursodeoxycholic acid regulates bile acids level and alters gut microbiota and glycolipid metabolism to attenuate diabetes. Gut Microbes. 2023;15(1):2192155. doi:10.1080/19490976.2023.2192155
8. Rowe JC, Summers SC, Quimby JM, Winston JA. Fecal bile acid dysmetabolism and reduced ursodeoxycholic acid correlate with novel microbial signatures in feline chronic kidney disease. Front Microbiol. 2024;15:1458090. doi:10.3389/fmicb.2024.1458090
9. Collins SL, Stine JG, Bisanz JE, Okafor CD, Patterson AD. Bile acids and the gut microbiota: metabolic interactions and impacts on disease. Nat Rev Microbiol. 2023;21(4):236–47. doi:10.1038/s41579-022-00805-x
10. Liu P, Jin M, Hu P, Sun W, Tang Y, Wu J, et al. Gut microbiota and bile acids: metabolic interactions and impacts on diabetic kidney disease. Curr Res Microb Sci. 2024;7:100315. doi:10.1016/j.crmicr.2024.100315
11. American Diabetes A. 2. classification and diagnosis of diabetes: standards of medical care in diabetes-2020. Diabetes Care. 2020;43:S14–S31. doi:10.2337/dc20-S002
12. Levey AS, Stevens LA, Schmid CH, Zhang Y, Castro III AF, Feldman HI, et al. A new equation to estimate glomerular filtration rate. Ann Intern Med. 2009;150(9):604–12. doi:10.7326/0003-4819-150-9-200905050-00006
13. Farris AB, Adams CD, Brousaides N, Della Pelle PA, Collins AB, Moradi E, et al. Morphometric and visual evaluation of fibrosis in renal biopsies. J Am Soc Nephrol. 2011;22(1):176–86. doi:10.1681/ASN.2009091005
14. Sakashita M, Tanaka T, Inagi R. Metabolic changes and oxidative stress in diabetic kidney disease. Antioxidants. 2021;10(7):1143. doi:10.3390/antiox10071143
15. Yuan Y, Huang L, Yu L, Yan X, Chen S, Bi C, et al. Clinical metabolomics characteristics of diabetic kidney disease: a meta-analysis of 1875 cases with diabetic kidney disease and 4503 controls. Diabetes Metab Res Rev. 2024;40(3):e3789. doi:10.1002/dmrr.3789
16. Wang XX, Wang D, Luo Y, Myakala K, Dobrinskikh E, Rosenberg AZ, et al. FXR/TGR5 dual agonist prevents progression of nephropathy in diabetes and obesity. J Am Soc Nephrol. 2018;29(1):118–37. doi:10.1681/ASN.2017020222
17. Watanabe M, Houten SM, Mataki C, Christoffolete MA, Kim BW, Sato H, et al. Bile acids induce energy expenditure by promoting intracellular thyroid hormone activation. Nature. 2006;439(7075):484–9. doi:10.1038/nature04330

18. Kaya D, Kaji K, Tsuji Y, Yamashita S, Kitagawa K, Ozutsumi T, et al. TGR5 activation modulates an inhibitory effect on liver fibrosis development mediated by anagliptin in diabetic rats. Cells. 2019;8(10):1153. doi:10.3390/cells8101153
19. Yang Z, Xiong F, Wang Y, Gong W, Huang J, Chen C, et al. TGR5 activation suppressed S1P/S1P2 signaling and resisted high glucose-induced fibrosis in glomerular mesangial cells. Pharmacol Res. 2016;111:226–36. doi:10.1016/j.phrs.2016.05.035
20. Chen C, Zhang B, Tu J, Peng Y, Zhou Y, Yang X, et al. Discovery of 4-aminophenylacetamide derivatives as intestine-specific farnesoid X receptor antagonists for the potential treatment of nonalcoholic steatohepatitis. Eur J Med Chem. 2024;264:115992. doi:10.1016/j.ejmech.2023.115992
21. Dehondt H, Marino A, Butruille L, Mogilenko DA, Loubota AC, Chavez-Talavera O, et al. Adipocyte-specific FXR-deficiency protects adipose tissue from oxidative stress and insulin resistance and improves glucose homeostasis. Mol Metab. 2023;69:101686. doi:10.1016/j.molmet.2024.101961
22. Hasan IH, Shaheen SY, Alhusaini AM, Mahmoud AM. Simvastatin mitigates diabetic nephropathy by upregulating farnesoid X receptor and Nrf2/HO-1 signaling and attenuating oxidative stress and inflammation in rats. Life Sci. 2024;340:122445. doi:10.1016/j.lfs.2024.122445
23. Balint L, Socaciu C, Socaciu AI, Vlad A, Gadalean F, Bob F, et al. Metabolites potentially derived from gut microbiota associated with podocyte, proximal tubule, and renal and cerebrovascular endothelial damage in early diabetic kidney disease in T2DM patients. Metabolites. 2023;13(8):893. doi:10.3390/metabo13080893
24. Balint L, Socaciu C, Socaciu AI, Vlad A, Gadalean F, Bob F, et al. Quantitative, targeted analysis of gut microbiota derived metabolites provides novel biomarkers of early diabetic kidney disease in type 2 diabetes mellitus patients. Biomolecules. 2023;13(7):1086. doi:10.3390/biom13071086
25. Zuo K, Fang C, Gao Y, Fu Y, Wang H, Li J, et al. Suppression of the gut microbiota–bile acid– FGF19 axis in patients with atrial fibrillation. Cell Prolif. 2023;56(11):e13488. doi:10.1111/cpr.13488
26. Choi H, Bae SJ, Choi G, Lee H, Son T, Kim JG, et al. Ninjurin1 deficiency aggravates colitis development by promoting M1 macrophage polarization and inducing microbial imbalance. FASEB J. 2020;34(6):8702–20. doi:10.1096/fj.201902753R
27. Luo Z, Xu J, Gao Q, Wang Z, Hou M, Liu Y, et al. Study on the effect of licochalcone A on intestinal flora in type 2 diabetes mellitus mice based on 16S rRNA technology. Food Funct. 2023;14(19):8903–21. doi:10.1039/d3fo00861d
28. Dong W, Zhao Y, Li X, Huo J, Wang W, et al. Corn silk polysaccharides attenuate diabetic nephropathy through restoration of the gut microbial ecosystem and metabolic homeostasis. Front Endocrinol. 2023;14:1232132. doi:10.3389/fendo.2023.1232132
29. Yang JY, Lee YS, Kim Y, Lee SH, Ryu S, Fukuda S, et al. Gut commensal Bacteroides acidifaciens prevents obesity and improves insulin sensitivity in mice. Mucosal Immunol. 2017;10(1):104–16. doi:10.1038/mi.2016.42
30. Shen Q, Zhong YT, Liu XX, Hu JN, Qi SM, Li K, et al. Platycodin D ameliorates hyperglycaemia and liver metabolic disturbance in HFD/STZ-induced type 2 diabetic mice. Food Funct. 2023;14(1):74–86. doi:10.1039/d2fo03308a
31. Cheng W, Zhou X, Jin C, Wu J, Xia Y, Lu M, et al. Acid-base transformative HADLA micelles alleviate colitis by restoring adaptive immunity and gut microbiome. J Control Release. 2023;364:283–96. doi:10.1016/j.jconrel.2023.10.039
32. Nakamoto N, Sasaki N, Aoki R, Miyamoto K, Suda W, Teratani T, et al. Gut pathobionts underlie intestinal barrier dysfunction and liver T helper 17 cell immune response in primary sclerosing cholangitis. Nat Microbiol. 2019;4(3):492–503. doi:10.1038/s41564-018-0333-1
33. van Nierop FS, Scheltema MJ, Eggink HM, Pols TW, Sonne DP, Knop FK, et al. Clinical relevance of the bile acid receptor TGR5 in metabolism. Lancet Diabetes Endocrinol. 2017;5(3):224–33. doi:10.1016/S2213-8587(16)30155-3
34. Lefebvre P, Cariou B, Lien F, Kuipers F, Staels B. Role of bile acids and bile acid receptors in metabolic regulation. Physiol Rev. 2009;89(1):147–91. doi:10.1152/physrev.00010.2008